

**Power Density Limits of Propulsion Motor for Electric Aircraft  
A Study on Insulation Thickness**

Wang, Jundong; Dong, Jianning; Niasar, Mohamad Ghaffarian; Zhu, Gangwei; Bauer, Pavol

**DOI**

[10.1109/ICEM60801.2024.10700069](https://doi.org/10.1109/ICEM60801.2024.10700069)

**Publication date**

2024

**Document Version**

Final published version

**Published in**

2024 International Conference on Electrical Machines, ICEM 2024

**Citation (APA)**

Wang, J., Dong, J., Niasar, M. G., Zhu, G., & Bauer, P. (2024). Power Density Limits of Propulsion Motor for Electric Aircraft: A Study on Insulation Thickness. In *2024 International Conference on Electrical Machines, ICEM 2024* (2024 International Conference on Electrical Machines, ICEM 2024). IEEE.  
<https://doi.org/10.1109/ICEM60801.2024.10700069>

**Important note**

To cite this publication, please use the final published version (if applicable).  
Please check the document version above.

**Copyright**

Other than for strictly personal use, it is not permitted to download, forward or distribute the text or part of it, without the consent of the author(s) and/or copyright holder(s), unless the work is under an open content license such as Creative Commons.

**Takedown policy**

Please contact us and provide details if you believe this document breaches copyrights.  
We will remove access to the work immediately and investigate your claim.

***Green Open Access added to TU Delft Institutional Repository***

***'You share, we take care!' - Taverne project***

**<https://www.openaccess.nl/en/you-share-we-take-care>**

Otherwise as indicated in the copyright section: the publisher is the copyright holder of this work and the author uses the Dutch legislation to make this work public.

# Power Density Limits of Propulsion Motor for Electric Aircraft: A Study on Insulation Thickness

Jundong Wang, Jianning Dong, Mohamad Ghaffarian Niasar, Gangwei Zhu, Pavol Bauer

Department of Electrical Engineering, Mathematics and Computer Science

Delft University of Technology, Delft, the Netherlands

Email: J.Wang-16@tudelft.nl

**Abstract**—This paper studies the power density limits of propulsion motor for electric aircraft considering thermal aspects and breakdown voltage reduction of insulation. The study employs multi-objective optimization (MOO) to explore various motor cooling options and filter configurations. The results show that motors with direct winding heat exchanger (DWHE) can reach higher specific power, while those equipped with water jacket cooling (WJC) offer a moderate design with simpler structure. Furthermore, the impact of sine wave and  $dv/dt$  filters on electric motors design is studied. The findings demonstrate that  $dv/dt$  filters enable designs with higher overall specific power compared to sine wave filters. Through simulations, this study identifies the challenge faced by aviation motor design in significantly increased insulation thickness, necessitating advanced insulation materials with a minimum thermal conductivity of 5 W/(m·K) to facilitate a high specific power design. Based on this assumption, a preliminary design of 9.6 kW/kg with an efficiency of 98% is presented.

**Index Terms**—electric aircraft, partial discharge, motor insulation, multi-objective optimization

## I. INTRODUCTION

To address the challenge of environmental impacts, Europe's aviation sector has introduced a set of sustainable initiatives targeting net-zero CO<sub>2</sub> emissions for all flights originating within and departing from the EU and the UK by 2050. The electrification of aircraft is currently the most promising alternative to meet the rising demand for air transportation while addressing economic and environmental concerns.

Transitioning toward electric propulsion (EP) systems for regional aircraft presents significant challenges due to severe environments at high altitudes and high power density demands. To address these challenges, extensive efforts have been devoted to the design of aircraft EP system, by replacing traditional engines with electric machines [1]. Among the various types of electric machines, Permanent magnet synchronous motor (PMSM) stands out due to its high power torque densities and superior efficiency, making it an ideal candidate for aerospace applications [2].

The winding structure of PMSM has various configurations. Fractional slot concentrated winding (FSCW) can reduce the possibility of phase-to-phase faults and limits short-circuit current due to its high phase inductance [3]. The winding layer of FSCW impacts motor performance. The double-layer winding offers improved harmonic performance over single-layer winding [4], at the cost of inferior electrical and thermal isolation. A megawatt-level radial flux (RF) surface-mounted

permanent magnet synchronous motor (SPMSM) designed for aircraft EP system is reported in [5]. Hence, RF double-layer FSCW SPMSM is selected for further study in this research.

Designing motors in aircraft EP systems faces a significant challenge in thermal management. Water jacket cooling (WJC) is a preferable option in engineering applications as it does not interfere with the internal electromagnetic structure [6]. However, in low and medium speed motors, a considerable amount of loss occurs within the winding, hindered by the long thermal transfer path from the winding to the water jacket. Several enhanced heat dissipation designs have been proposed to effectively cool the winding [7]–[9]. Among these designs, direct winding heat exchanger (DWHE) reaches a balance between system complexity and cooling efficiency. Aggressive cooling designs, such as completely flooded stator [10], may encounter heterogeneous thermal expansion during operation at different altitudes, leading to safety issues. As a result, WJC and DWHE are selected as cooling options for further investigation in this study. Fig. 1 demonstrates RF Double-layer FSCW SPMSM with inner rotor (IR) and outer rotor (OR) structure, incorporating these two cooling options. The performance of these four motor configurations will be examined in section III.

One major challenge in dissipating winding loss lies in the system insulation. Thicker insulation layers are required at high altitudes to prevent partial discharge (PD) occurrences, which influences the lifetime of insulation materials. Partial discharge inception voltage (PDIV) is primarily determined by air pressure and the diameter of air cavities inside insulation.

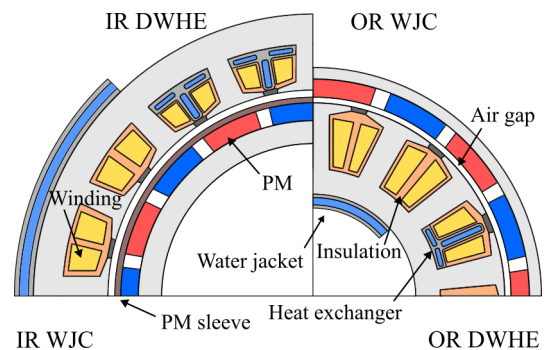


Fig. 1. PMSM configurations.

At 10,000 meters, low air pressure can decrease the PDIV by 50% [11]. Furthermore, recent studies highlight the impact of wide bandgap power electronics on insulation stress due to high  $dv/dt$  [12]. Additionally, the rising power demands of EP system escalates voltage levels, further increasing the need for thicker insulation. Medium voltage DC (MVDC) powertrain architectures have been identified as enablers for EP powertrains in large-body aircraft with multi-megawatt requirements [13]. However, the impact of insulation on aviation motor design has not received adequate attention in recent research.

In addition to air pressure and voltage levels, output filters of inverters play a crucial role in motor insulation design. Typically, there are two types of output filters:  $dv/dt$  filters [14] and sine wave filters [15] (See Fig. 2). While  $dv/dt$  filters are lighter than sine wave filters, they impose higher voltage stress across motor insulation, demanding for thicker insulation layer and potentially increasing the overall weight.

Hence, to investigate the influence of insulation on aircraft EP motor design, the main points of this paper are outlined as follows:

- A new calculation approach for estimating insulation thickness on aviation motors is proposed based on experiment data from previous research.
- A multi-objective optimization (MOO) design of motors and filters is analyzed. Furthermore, the combined design of these two is demonstrated with various topologies.

The rest of this paper is structured as follows: Section II provides an analysis of insulation-related experiment results from previous research and formulates a method for calculating the thickness of insulation layers. Then, section III provides studies of motors and filters based on the equation introduced in section II. Finally, section IV concludes this paper.

## II. SPECIFICATIONS ON MOTOR INSULATION

### A. Motor Fed by Sine Wave Filter

The insulation layer between the motor winding and stator is composed of many components, as illustrated in Fig. 3. Small air cavities can be found within these layers, especially in resin impregnation, where PD might occur and degrade dielectric strength, contributing to insulation failure. The size

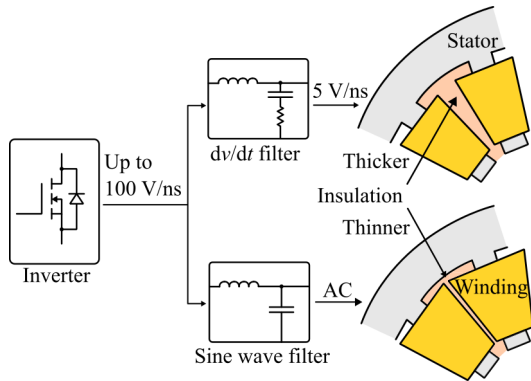


Fig. 2. Influence of filters on motor insulation.

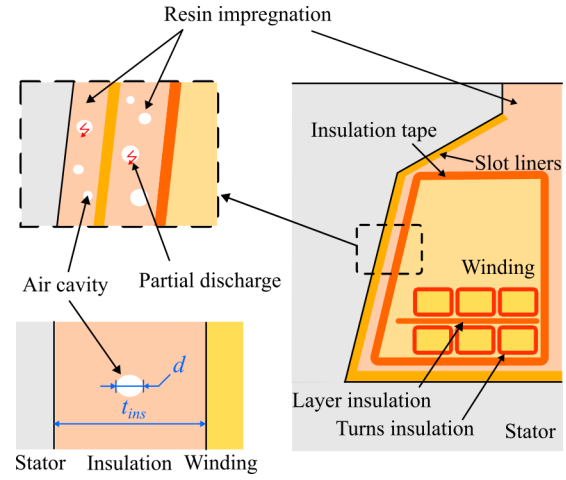


Fig. 3. Components of motor insulation.

of air cavity  $d$ , along with air pressure  $p$ , determine the PDIV according to Paschen's law. A simplified Paschen curve equation derived from experimental data [17] is expressed by

$$V_b = 24.36p \cdot d + 6.72\sqrt{p \cdot d} \quad (1)$$

where  $V_b$  denotes the breakdown voltage. Defining  $U$  as the voltage applied between the winding and stator core, the electric field strength in air cavity  $E_{\text{air}}$  and insulation material  $E_{\text{ins}}$  are in terms of

$$\begin{aligned} E_{\text{air}} &= \frac{U \cdot \epsilon_{\text{ins}}}{d \cdot \epsilon_{\text{ins}} + (t_{\text{ins}} - d)\epsilon_{\text{air}}} \\ E_{\text{ins}} &= \frac{U \cdot \epsilon_{\text{air}}}{d \cdot \epsilon_{\text{ins}} + (t_{\text{ins}} - d)\epsilon_{\text{air}}} \end{aligned} \quad (2)$$

where  $\epsilon_{\text{air}}$  and  $\epsilon_{\text{ins}}$  represent the relative permittivity of air and insulation material, respectively. To note that (2) is based on parallel plate capacitor assumption. Therefore, the thickness of insulation  $t_{\text{ins}}$ , as illustrated in Fig. 3, is determined as:

$$t_{\text{ins}} = \frac{U \cdot \epsilon_{\text{ins}}}{E_{\text{air}} \cdot \epsilon_{\text{air}}} - \frac{t_{\text{air}}(\epsilon_{\text{ins}} - \epsilon_{\text{air}})}{\epsilon_{\text{air}}} \quad (3)$$

To avoid PD occurrences,  $E_{\text{air}}$  is constrained as:

$$E_{\text{air}} = \frac{K_s \cdot V_b}{d} \quad (4)$$

where  $K_s$  is a positive scale factor bounded between 0 and 1. Further substituting (1) and (4) into (3) provides the insulation thickness for sine wave filter-fed motors.

### B. Motor Fed by $dv/dt$ Filter

The terminal voltage of a  $dv/dt$  filter-fed motor exhibits a high-frequency repetitive pulse pattern where the Paschen curve in (1) does not fit anymore [18]. To address this deviation, an experimental-based model was proposed in [18] to predict repetitive partial discharge inception voltage (RPDIV), resulting in the modified equation:

$$V_b^m = 24.36p \cdot d + 0.48\sqrt{p \cdot d} \quad (5)$$

The superscript ‘ $m$ ’ in  $V_b^m$  denotes the modification of the Paschen curve. It’s worth noting that under high-frequency voltage supply ( $>5$  kHz), the difference between PDIV and RPDIV can be neglected [18].

Following the same methodology as (2) to (4), a recommended insulation thickness can be derived. However, experiments reported in [19] indicate that simply replicating the calculation method, the insulation lifetime of  $dv/dt$  filter-fed motors is significantly reduced compared to sine wave filter-fed motors. Therefore, further procedures should be developed to compensate for the difference in life expectancy.

Experiment results from [20] illustrate that the lifetime of tested insulation fed by 5 kHz, 60 V/ns bipolar repetitive square wave voltage, is approximately 35 minutes, denoted as  $T_{5\text{kHz},60\text{V/ns}}$ . Meanwhile, another tested sample fed by 1 kHz, bipolar AC voltage has a lifetime of around 280 minutes, marked as  $T_{1\text{kHz},\text{AC}}$ . What’s more, a mathematical model is summarized in [19] based on experimental data to estimate the lifetime of tested insulation materials. The lifetime  $T_{f,dv/dt}$  is given by:

$$T_{f,dv/dt} = T_{\text{ref}} \left( \frac{f_{\text{ref}}}{f} \right)^{1.25} \left( \frac{dv/dt_{\text{ref}}}{dv/dt} \right)^{\frac{f_s}{128000}} \quad (6)$$

where  $T_{\text{ref}}$  represents the reference lifetime, and  $f_{\text{ref}}$  is the reference frequency set at 50 kHz, while  $dv/dt_{\text{ref}}$  denotes reference  $dv/dt$  ratio of 30 V/ns.  $f$  and  $dv/dt$  refers to the frequency and voltage rising ratio of interest, respectively.

Considering a  $dv/dt$  filter with an output voltage rising/falling ratio of  $dV/dT$  and a switching frequency of  $f_s$ , the lifetime ratio of  $T_{1\text{kHz},\text{AC}}$  to that of  $dv/dt$  filter is given by

$$\begin{aligned} N &= \frac{T_{1\text{kHz},\text{AC}}}{T_{f_s,dV/dT}} \\ &= \frac{T_{1\text{kHz},\text{AC}}}{T_{5\text{kHz},60\text{V/ns}}} \frac{T_{5\text{kHz},60\text{V/ns}}}{T_{f_s,dV/dT}} \\ &= \frac{280}{35} \left( \frac{f_s}{5\text{kHz}} \right)^{1.25} \left( \frac{30\text{V/ns}}{60\text{V/ns}} \right)^{\frac{f_s}{128}} \left( \frac{dV/dT}{30\text{V/ns}} \right)^{\frac{f_s}{128000}} \end{aligned} \quad (7)$$

where the variables  $f_s$  and  $dV/dT$  are set within the ranges of  $f_s \in [10\text{kHz}, 50\text{kHz}]$  and  $dV/dT \in [1\text{V/ns}, 60\text{V/ns}]$ , aligning with extrapolation boundary of experiments. This results in a difference in life expectancy denoted by  $N$ . To compensate for the lifetime loss, the electric field strength in air cavity  $E_{\text{air}}$  should be reduced to a certain value  $E_{\text{air}}^{\text{comp}}$ . Reference [21] established an inverse power law model to estimate lifetime as:

$$T_{50\text{kHz},2\text{V/ns}} = K_c \left( \frac{E}{E_0} \right)^{-37.5} \quad (8)$$

where  $K_c$  represents a lifetime constant, and  $E_0$  has a unit of electric field strength. Given  $f_s$  and  $dV/dT$ , the lifetime model (8) can be extended to calculate  $E_{\text{air}}^{\text{comp}}$ , which is given by:

$$E_{\text{air}}^{\text{comp}} = E_{\text{air}} \cdot N^{-\frac{1}{37.5}}. \quad (9)$$

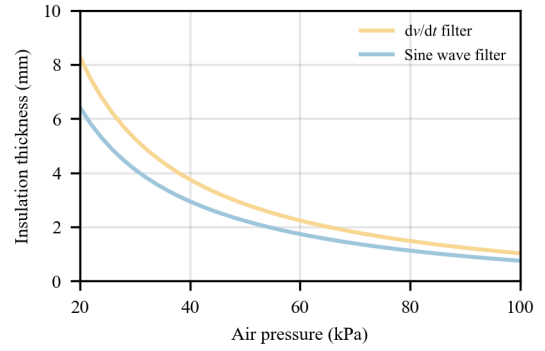


Fig. 4. Relationship between insulation thickness and air pressure.

Finally, to avoid PD occurrences and extend the insulation lifetime, the insulation thickness  $t_{\text{ins}}$  of a motor fed by a  $dv/dt$  filter is specified as:

$$t_{\text{ins}} = \frac{U \cdot \epsilon_{\text{ins}}}{E_{\text{air}}^{\text{comp}} \cdot \epsilon_{\text{air}}} - \frac{t_{\text{air}}(\epsilon_{\text{ins}} - \epsilon_{\text{air}})}{\epsilon_{\text{air}}}. \quad (10)$$

In a scenario where the insulation design with  $d = 200 \mu\text{m}$ , bipolar DC bus  $U = \pm 400$  V, inverter switching frequency  $f_s = 40$  kHz, motor fundamental electric frequency  $f_s = 1$  kHz and scale factor  $K_s = 0.5$ , the motor phase-to-ground insulation thickness  $t_{\text{ins}}^{\text{sin}}$  and  $t_{\text{ins}}^{\text{dv/dt}}$ , when fed by sine wave and  $dv/dt$  filter respectively, are calculated under different air pressures. The results are depicted in Fig. 4. At ground level ( $p = 100$  kPa),  $t_{\text{ins}}^{\text{sin}} = 0.74$  mm and  $t_{\text{ins}}^{\text{dv/dt}} = 1.02$  mm. At aircraft cruising altitude ( $p \approx 22$  kPa),  $t_{\text{ins}}^{\text{sin}} = 5.80$  mm and  $t_{\text{ins}}^{\text{dv/dt}} = 7.45$  mm, indicating a 7.8 and 7.3 times increase respectively compared to sea level. Hence, the insulation layer of motor will change significantly in aircraft EP applications compared to ground-level counterparts. This change will bring potential influence on motor design, as elaborated in the next section.

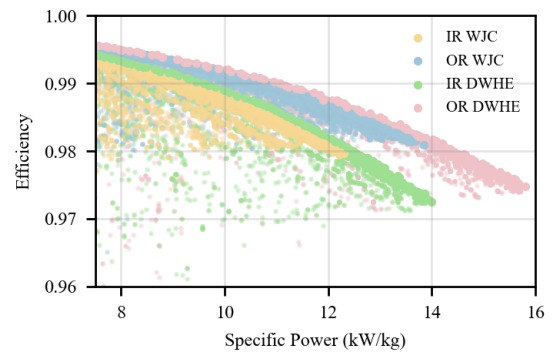


Fig. 5. MOO results of ground-level motors.

TABLE I  
DESIGN SPECIFICATIONS AND CONSTRAINTS ON ELECTRIC MOTORS

Parameters	Value	Unit
Shaft power	1355	kW
Shaft RPM	950	-
Bus voltage	$\pm 400$	V
Ambient temperature	40	$^{\circ}\text{C}$
Coolant inlet temperature	50	$^{\circ}\text{C}$
Maximum coolant temperature-rise	20	$^{\circ}\text{C}$
Maximum winding temperature-rise	140	$^{\circ}\text{C}$
Coolant mass flow	90	L/min
Maximum coolant pressure drop across the motor	25	kPa

### III. MOO BASED POWER DENSITY LIMIT EXPLORATION OF MOTORS AND FILTERS

The aim of MOO in EP systems is to achieve the highest efficiency while minimizing the weight. However, the optimization process presents more challenges when it involves interactions among multiple components. For instance, the selection of an inverter output filter will influence the motor design, and vice versa. Joint optimization efforts must carefully consider the interaction between each local parts. Section III-A presents a comparative analysis between ground-level and aviation-level motors, while section III-B performs an optimization of sine wave and  $dv/dt$  filters to highlight their differences in weigh and loss. Finally, the results of joint optimization, combining motor and filter, are detailed in section III-C.

#### A. Motors Optimization

This study focuses on motor optimization according to the specific design requirements listed in Table. I. A water/glycol mixture (50% water, 50% glycol) is chosen as coolant, regarding its successful application in electric vehicles. The motor core employs iron cobalt vanadium alloy (FeCoV) as the soft magnet material. The selected motor structure is an RF double-layer FSCW SPMSM with a pole/slot pair of 10/12. To enhance fault-tolerance capability [16] and reduce phase current, five element motors are connected in parallel, resulting in a total pole/slot configuration of 50/60. WJC and DWHE cooling options, combined with OR and IR structure yields

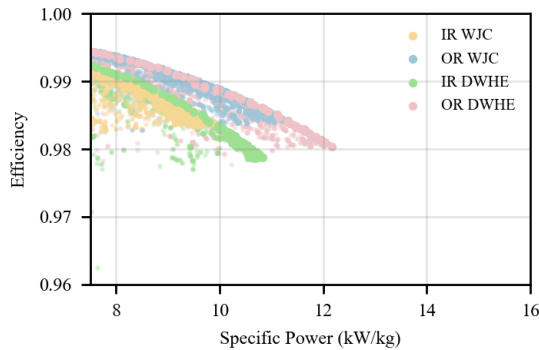


Fig. 6. MOO results of aviation-level motors.

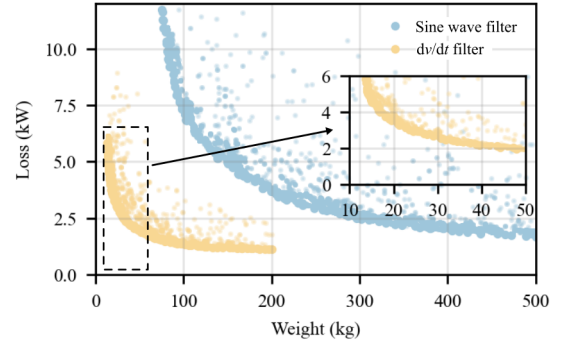


Fig. 7. MOO results of sine wave and  $dv/dr$  filters.

four motor topology combinations as depicted in Fig. 1. The design space for MOO algorithm are outlined in Table. I. To note that the air gap length of IR motor is larger than that of OR motor due to the PM sleeve.

Electromagnetic part of the motor is modeled by adopting magnetic equivalent circuit (EMC). Thermal modeling is achieved through the lumped-parameter thermal network (LPTN), with specifications detailed in [22]. The MOO results for ground-level design are illustrated in Fig. 5. The weight includes active parts of the motor and the cooling jacket (WJC) or channel (DWHE). The losses include winding loss, stator core loss and rotor windage loss. Based on the results, OR structure demonstrates higher power density compared to IR structure, owing to a smaller air gap length and a more compact stator structure. On the other hand, the advantage of direct contact with winding makes the motor equipped with DWHE cooling reach higher specific power than those surrounded by WJC. The highest specific power in ground-level design can approximate 16 kW/kg. Notably, the limit of specific power is the winding temperature-rise, as the coolant has not reached its maximum allowed temperature. Since the thermal conductivity of motor insulation material is around 0.5 W/(m·K). The motor encounter sever performance degradation at high altitudes. As depicted in Fig. 6, the specific power stops at 12 kW/kg when the winding temperature-rise reaches the limit. Considering the additional weight of shafts, bearings, housing and other supporting facilities [25], the specific power

TABLE II  
MOO DESIGN SPACE FOR ELECTRIC MOTORS

Parameters	Value	Unit
Motor outer diameter	0.5 - 1.2	m
Split ratio	0.7 - 0.95	-
Length to diameter ratio	0.2 - 1.0	-
Slot space ratio	0.6 - 0.95	-
Slot depth ratio	0.6 - 0.95	-
Air gap length of OR structure	1.5 - 3.5	mm
Air gap length of IR structure	2.5 - 3.5	mm
PM thickness	5 - 15	mm
Pole shoes coefficient	0.2 - 0.7	-
Pole-arc coefficient	$2\pi/3 - 5\pi/6$	-
Cooling channel height	4 - 10	mm



TABLE III  
DESIGN SPECIFICATIONS ON FILTERS

Parameters	Value	Unit
Rated power	1355	kVA
Switching frequency	40	kHz
$dv/dt$ limit	5	V/ns
Current ripple	5%	-
Cooling air speed	10	m/s

including non active component would drop to around 5 kW/kg and the motor will be too heavy for the integration into aircraft EP systems. Thus, aviation motor design necessitates advanced insulation materials with high thermal conductivity up to 5 W/(m·K). Subsequent designs in this paper will be based on this assumption.

### B. Filters Optimization

The design parameters for sine wave and  $dv/dt$  filters are provided in Table. III. For parameters calculation procedures can be referenced in [23]. The thermal network model is similar to that used in [22], as the double-E core structure is chosen for the inductance. Nanocrystalline powder is selected as the core material for its high saturation flux density and low hysteresis loss, with core loss data obtained from [24]. The optimization results are presented in Fig. 7, showing that the loss and mass of the sine wave filter are higher than those of the  $dv/dt$  filter due to the larger required inductance value. However, connecting the motor to the sine wave filter can decrease the motor insulation thickness by 22%, thereby benefiting the motor design and reducing the motor weight. Consequently, the overall weight of the motor and sine wave filter may be lower than that of the motor and  $dv/dt$  filter, suggesting further study for a joint optimization combining the motor and passive filter.

### C. Joint Optimization for Motors and Filters

The findings depicted in Fig. 5 suggest that the OR structure outperforms the IR structure. Therefore, in joint optimization process, the OR structure is selected, integrating WJC and DWHE cooling facilities, together with sine wave and  $dv/dt$  filters.

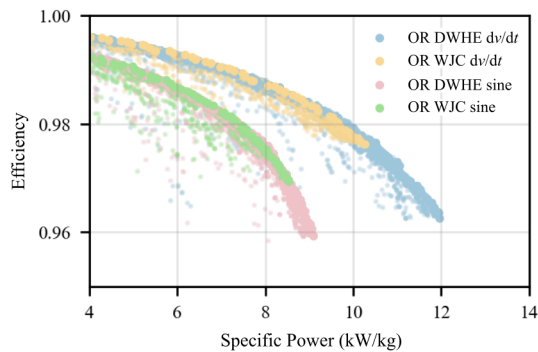


Fig. 8. Joint MOO results of motors and filters.

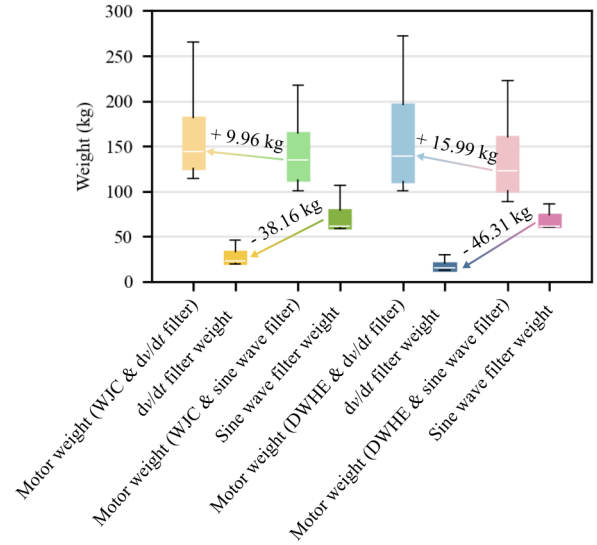


Fig. 9. Weight specifications on joint MOO results.

Fig. 8 presents the MOO outcomes. Analysis of the results indicates that motors connected to  $dv/dt$  filter result in higher overall power density compared to those connected to sine wave filters. The Pareto front of WJC and DWHE largely overlaps, except for high specific power areas. Further insights into these results are provided in Fig. 9. Regarding motor equipped with WJC, connecting to a  $dv/dt$  filter results in a median weight increases of 9.96 kg due to the thicker insulation layers. However, the  $dv/dt$  filter itself is 38.16 kg lighter than the sine wave filter, resulting in a net system weight reduction of 28.2 kg. This weight saving is also observed for motors equipped with DWHE. Consequently, the increased weight associated with the sine wave filter does not offset the decreased weight of the motor when compared to  $dv/dt$  filter.

Fig. 10 offers a breakdown of the mass for a RF double-layer FSCW OR SPMSM with WJC connected to a  $dv/dt$  filter, achieving an overall efficiency of 98% and a specific power of 9.6 kW/kg. Notably, system insulation, including motor's and filter's, accounts for 11.67% of the total mass, suggesting the challenge when transitioning motors from ground-level to aviation-level.

## IV. CONCLUSIONS

This paper develops an algorithm based on previous experimental data to calculate the insulation thickness of aviation motors. A MOO methodology is developed to explore the physical limits of motor and its filter. The results indicate a substantial increase in the thickness of aviation motor insulation layer, with a factor of 7.8 (when fed by sine wave filter) and 7.3 (when fed by  $dv/dt$  filter) compared to ground-level conditions, considering an air cavity of 200  $\mu\text{m}$ . Furthermore, two cooling options, WJC and DWHE, are investigated. It's found that DWHE enables a higher specific power design, while WJC offers a moderate design with

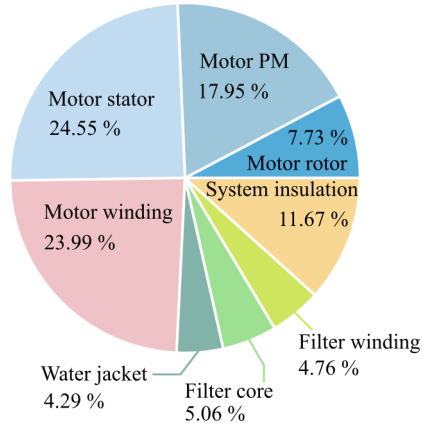


Fig. 10. Mass breakdown of the designed motor and filter.

simpler structure. Furthermore, this study explore the influence of passive filter selection on motor design. Despite inducing a thicker motor insulation layer,  $dv/dt$  filters demonstrates superior performance over sine wave filters, leading to a net reduction in overall system weight.

#### ACKNOWLEDGMENT

This research is co-funded by the HERA project, which has received funding from the European Union under grant agreement No. 101102007.

#### REFERENCES

- [1] E. Sayed et al., "Review of Electric Machines in More-/Hybrid-/Turbo-Electric Aircraft," in *IEEE Transactions on Transportation Electrification*, vol. 7, no. 4, pp. 2976-3005, Dec. 2021.
- [2] J. A. Rosero, J. A. Ortega, E. Aldabas and L. Romeral, "Moving towards a more electric aircraft," *IEEE Aerospace and Electronic Systems Magazine*, vol. 22, p. 3-9, March 2007.
- [3] M. D. Pre, "Analysis and design of fault-tolerant drives," Ph.D. dissertation, Dept. Elect. Eng., Univ. Padova, Italy, Jan. 2008.
- [4] N. Bianchi, S. Bolognani, M. D. Pre and G. Grezzani, "Design considerations for fractional-slot winding configurations of synchronous machines," *IEEE Transactions on Industry Applications*, vol. 42, p. 997-1006, July 2006.
- [5] H. Andersen, Y. Chen, M. M. Qasim, D. G. Cuadrado, D. M. Otten, E. Greitzer, D. J. Perreault, J. L. Kirtley, J. H. Lang and Z. Spakovszky, "Design and Manufacturing of a High-Specific-Power Electric Machine for Aircraft Propulsion," *MIT News*, 2023.
- [6] C. Dong, Y. Qian, Y. Zhang and W. Zhuge, "A Review of Thermal Designs for Improving Power Density in Electrical Machines," in *IEEE Transactions on Transportation Electrification*, vol. 6, no. 4, pp. 1386-1400, Dec. 2020.
- [7] W. Sixel, M. Liu, G. Nellis and B. Sarlioglu, "Ceramic 3-D Printed Direct Winding Heat Exchangers for Thermal Management of Concentrated Winding Electric Machines," in *IEEE Transactions on Industry Applications*, vol. 57, no. 6, pp. 5829-5840, Nov.-Dec. 2021.
- [8] F. R. Ismagilov, V. E. Vavilov and D. V. Gusakov, "Design Features of Liquid-Cooled Aviation Starter Generators," in *2018 IEEE International Conference on Electrical Systems for Aircraft, Railway, Ship Propulsion and Road Vehicles & International Transportation Electrification Conference (ESARS-ITEC)*, 2018.
- [9] Y. Xie, L. Chen, X. Wang, J. Zhang, F. Leonardi, B. M. Sung, A. R. Munoz and M. W. Degner, "In-slot Direct Cooling Design and Optimization for Electric Machines," in *2021 IEEE International Electric Machines & Drives Conference (IEMDC)*, 2021.
- [10] F. R. Ismagilov, V. E. Vavilov and D. V. Gusakov, "Design Features of Liquid-Cooled Aviation Starter Generators," in *2018 IEEE International Conference on Electrical Systems for Aircraft, Railway, Ship Propulsion and Road Vehicles & International Transportation Electrification Conference (ESARS-ITEC)*, 2018.
- [11] I. Cotton, R. Gardner, D. Schweickart, D. Grosean and C. Severns, "Design considerations for higher electrical power system voltages in aerospace vehicles," in *2016 IEEE International Power Modulator and High Voltage Conference (IPMHVC)*, 2016.
- [12] B. Hu, Z. Wei, H. You, R. Na, R. Liu, H. Xiong, P. Fu, J. Zhang and J. Wang, "A Partial Discharge Study of Medium-Voltage Motor Winding Insulation Under Two-Level Voltage Pulses With High  $Dv/Dt$ ," *IEEE Open Journal of Power Electronics*, vol. 2, p. 225-235, 2021.
- [13] J. Benzaquen, J. He and B. Mirafzal, "Toward more electric powertrains in aircraft: Technical challenges and advancements," *CES Transactions on Electrical Machines and Systems*, vol. 5, p. 177-193, September 2021.
- [14] M. Haider, M. Guacci, D. Bortis, J. W. Kolar and Y. Ono, "Analysis and Evaluation of Active/Hybrid/Passive  $dv/dt$ -Filter Concepts for Next Generation SiC-Based Variable Speed Drive Inverter Systems," *2020 IEEE Energy Conversion Congress and Exposition (ECCE)*, Detroit, MI, USA, 2020, pp. 4923-4930.
- [15] P. Mishra and R. Maheshwari, "Design, Analysis, and Impacts of Sinusoidal LC Filter on Pulsewidth Modulated Inverter Fed-Induction Motor Drive," in *IEEE Transactions on Industrial Electronics*, vol. 67, no. 4, pp. 2678-2688, April 2020.
- [16] W. Cao, B. C. Mecrow, G. J. Atkinson, J. W. Bennett and D. J. Atkinson, "Overview of Electric Motor Technologies Used for More Electric Aircraft (MEA)," in *IEEE Transactions on Industrial Electronics*, vol. 59, no. 9, pp. 3523-3531, Sept. 2012.
- [17] E. Kuffel, W.S. Zaengl and J. Kuffel, *High voltage engineering – Fundamentals*, Oxford, U.K.:Newnes, 2000.
- [18] D. R. Meyer, A. Cavallini, L. Lusuardi, D. Barater, G. Pietrini and A. Soldati, "Influence of impulse voltage repetition frequency on RPDIv in partial vacuum," in *IEEE Transactions on Dielectrics and Electrical Insulation*, vol. 25, no. 3, pp. 873-882, June 2018.
- [19] R. Agarwal, H. Li, Z. Guo and P. Cheetham, "The Effects of PWM With High  $dv/dt$  on Partial Discharge and Lifetime of Medium-Frequency Transformer for Medium-Voltage (MV) Solid State Transformer Applications," in *IEEE Transactions on Industrial Electronics*, vol. 70, no. 4, pp. 3857-3866, April 2023.
- [20] P. Wang, A. Cavallini and G. C. Montanari, "The influence of repetitive square wave voltage parameters on enameled wire endurance," in *IEEE Transactions on Dielectrics and Electrical Insulation*, vol. 21, no. 3, pp. 1276-1284, June 2014.
- [21] P. Mathew, M. G. Niasar and P. Vaessen, "Design of High-Frequency Fast-Rise Pulse Modulators for Lifetime Testing of Dielectrics," in *IEEE Transactions on Dielectrics and Electrical Insulation*, vol. 30, no. 6, pp. 2798-2808, Dec. 2023.
- [22] D. Liang et al., "A Hybrid Lumped-Parameter and Two-Dimensional Analytical Thermal Model for Electrical Machines," in *IEEE Transactions on Industry Applications*, vol. 57, no. 1, pp. 246-258, Jan.-Feb. 2021.
- [23] H. Kim, B. -H. Kim and S. Bhattacharya, "An Analytical Design Strategy and Implementation of a  $Dv/Dt$  Filter for WBG Devices Based High Speed Machine Drives," *IECON 2018 - 44th Annual Conference of the IEEE Industrial Electronics Society*, Washington, DC, USA, 2018.
- [24] C. Jiang, X. Li, S. S. Ghosh, H. Zhao, Y. Shen and T. Long, "Nanocrystalline Powder Cores for High-Power High-Frequency Power Electronics Applications," in *IEEE Transactions on Power Electronics*, vol. 35, no. 10, pp. 10821-10830, Oct. 2020.
- [25] D. Golovanov, L. Papini, D. Gerada, Z. Xu and C. Gerada, "Multidomain Optimization of High-Power-Density PM Electrical Machines for System Architecture Selection," in *IEEE Transactions on Industrial Electronics*, vol. 65, no. 7, pp. 5302-5312, July 2018.

#### BIOGRAPHIES

**Jundong Wang** was born in Hefei, China, in 1998. He received the B.S. and M.S. degrees in electrical engineering from South East University, Nanjing, China, in 2020 and 2023, respectively. He is currently working on his Ph.D. in electrical



engineering at Delft University of Technology, Delft, The Netherlands. His main research interests include modeling and control of electric propulsion system for aircraft.

**Jianning Dong** received the B. S. and Ph.D. degrees in electrical engineering from Southeast University, Nanjing, China, in 2010 and 2015, respectively. He was a Post-Doctoral Researcher with the McMaster Automotive Resource Centre, McMaster University, Hamilton, ON, Canada. Since 2016, he has been an Assistant Professor with the DC System, Energy Conversion and Storage (DCE&S) Group, Delft University of Technology (TU Delft), Delft, The Netherlands. His research interests include electromechanical energy conversion and contactless power transfer.

**Mohamad Ghaffarian Niasar** was born in Tehran, Iran, in 1984. He received the M.Sc. degree in electrical power engineering from the Sharif University of Technology, Tehran, Iran, in 2008, and the Ph.D. degree in electrical engineering from the KTH Royal Institute of Technology, Stockholm, Sweden, in 2015. He is currently an Assistant Professor with High Voltage Technology Group, Technical University of Delft, Delft, The Netherlands. His main research interests include aging of electrical insulation, HVdc insulation system, partial discharges, high-voltage power electronics, high-frequency power transformers, power cables, and FEM modeling.

**Gangwei Zhu** was born in Hunan, China, in 1997. He received the B.S. degree in electrical engineering from Central South University, Changsha, China, in 2018, and the M.S. degree in electrical engineering from Shanghai Jiao Tong University, Shanghai, China, in 2021. He is currently working toward the Ph.D. degree in electrical engineering with the Delft University of Technology, Delft, The Netherlands. His research interests include advanced control and modulation for wireless power transfer.

**Pavol Bauer** received the master's degree in electrical engineering from the Technical University of Kosice, Košice, Slovakia, in 1985, and the Ph.D. degree from the Delft University of Technology, Delft, The Netherlands, in 1995.

He is currently a Full Professor with the Department of Electrical Sustainable Energy, Delft University of Technology, where he is also the Head of the DC Systems, Energy Conversion and Storage Group. He received the title prof. from the President of Czech Republic at the Brno University of Technology, Brno University of Technology, Brno, Czechia, in 2008, and the Delft University of Technology in 2016. From 2002 to 2003, he worked partially at KEMA (DNV GL), Arnhem, The Netherlands, on different projects related to power electronics applications in power systems. He is also an Honorary Professor with the Politehnica University Timișoara, Timișoara, Romania. He has worked on many projects for industry concerning wind and wave energy, and power electronic applications for power systems, such as Smarttrafo, and HVdc systems, projects for smart cities, such as PV charging of electric vehicles, PV and storage integration, contactless charging. He participated in several Leonardo da Vinci, H2020, and Electric Mobility Europe EU projects as a Project Partner (ELINA, INETELE, E-Pragmatic, Micact, Trolley 2.0,

and OSCD) and a Coordinator (PEMCWebLab.com-Edipe, SustEner, and Eranet DCMICRO). He has published over 95 journal articles and 350 conference papers in his field (with an H factor of 39 from Google Scholar and 29 from Web of Science). He is the author or a coauthor of eight books. He has organized several tutorials at international conferences. He holds nine international patents.

Dr. Bauer is also a member of the Executive Committee of the European Power Electronics Association (EPE) and international steering committees at numerous conferences. He is also the Former Chairperson of the Benelux IEEE Joint Industry Applications Society, Power Electronics and Power Engineering Society Chapter, and the Chairperson of the Power Electronics and Motion Control (PEMC) Council.